PNAS
Proceedings of the National Academy of Sciences of the United States of America www.pnas.org

A climate-change risk analysis for world ecosystems

Marko Scholze, Wolfgang Knorr, Nigel W. Arnell, and I. Colin Prentice

PNAS 2006;103;13116-13120; originally published online Aug 21, 2006;
doi:10.1073/pnas.0601816103

A climate-change risk analysis for world ecosystems

Marko Scholze*†, Wolfgang Knorr*, Nigel W. Arnell‡, and I. Colin Prentice*

*Quantifying and Understanding the Earth System (QUEST), Department of Earth Sciences, University of Bristol, Wills Memorial Building, Queen's Road, Bristol BS8 1RJ, United Kingdom; and ‡Tyndall Centre for Climate Change Research and School of Geography, University of Southampton, Southampton SO17 1BJ, United Kingdom

Edited by Christopher B. Field, Carnegie Institution of Washington, Stanford, CA, and approved July 10, 2006 (received for review March 6, 2006)

We quantify the risks of climate-induced changes in key ecosystem processes during the 21st century by forcing a dynamic global vegetation model with multiple scenarios from 16 climate models and mapping the proportions of model runs showing forest/nonforest shifts or exceedance of natural variability in wildfire frequency and freshwater supply. Our analysis does not assign probabilities to scenarios or weights to models. Instead, we consider distribution of outcomes within three sets of model runs grouped by the amount of global warming they simulate: <2°C (including simulations in which atmospheric composition is held constant, i.e., in which the only climate change is due to greenhouse gases already emitted), 2–3°C, and >3°C. High risk of forest loss is shown for Eurasia, eastern China, Canada, Central America, and Amazonia, with forest extensions into the Arctic and semiarid savannas; more frequent wildfire in Amazonia, the far north, and many semiarid regions; more runoff north of 50°N and in tropical Africa and northwestern South America; and less runoff in West Africa, Central America, southern Europe, and the eastern U.S. Substantially larger areas are affected for global warming >3°C than for <2°C; some features appear only at higher warming levels. A land carbon sink of ≈1 Pg of C per yr is simulated for the late 20th century, but for >3°C this sink converts to a carbon source during the 21st century (implying a positive climate feedback) in 44% of cases. The risks continue increasing over the following 200 years, even with atmospheric composition held constant.

climate change impacts | dangerous climate change | ecosystem vulnerability | ecosystem modeling

The objective of the United Nations Framework Convention on Climate Change (1) is to "achieve stabilization of greenhouse gas concentrations in the atmosphere at a level that would prevent dangerous anthropogenic interference with the climate system." This level should "allow ecosystems to adapt naturally to climate change" (1). But what is dangerous climate change, and how likely are different amounts of climate change to have major impacts on the world's ecosystems? In the scientific literature, "dangerous climate change" has often been interpreted in terms of critical levels of climate change or thresholds triggering abrupt climate-change events (2). However, there is mounting evidence for local ecological responses even to relatively minor climate changes that have occurred during recent decades (3). Much larger changes, compared with what has occurred already, are projected for the 21st century (4), yet future climate-change risks for ecosystems worldwide have generally been assessed only on qualitative scales, e.g., from "risks for some" to "risks for many" or from "very low" to "higher" (5). For example, a quantitative analysis has been carried out for the global probability of dangerous anthropogenic interference in a coupled social–natural system, which, however, does not involve spatially explicit climate modeling (6, 7).

We used outputs from 52 coupled atmosphere–ocean general circulation model (GCM) future scenario simulations modeled by 16 different GCMs as input to the Lund–Potsdam–Jena (LPJ) dynamic global vegetation model (8, 9) in an attempt to provide a more quantitative spatially resolved global assessment of climate-change-driven risks for world ecosystems. We calculated the risk of exceedance of critical levels of change for ecosystem type, wildfire frequency, and freshwater supply (runoff). Runoff is considered as an ecosystem property because transpiration and interception are influenced by biological processes and affected by CO_2 concentration as well as by climate (9). We also analyzed globally aggregated changes in the carbon balance of ecosystems.

We divided the 52 climate model scenario simulations into three groups according to the calculated increase in global mean surface temperature between 1961–1990 and 2071–2100. Global mean surface temperature is the "traditional" indicator for the degree of climate change; it is linked to the radiative forcing of the greenhouse gas emissions because it increases monotonically with emissions, and global mean temperature increase is largely monotonic with regional temperature increases. In every case, the risk is quantified as the number of model runs in which the critical change occurs, as a fraction of the total number of model runs in the group (for individual model results, see Figs. 3–6, which are published as supporting information on the PNAS web site).

Results

Changes in climate affect photosynthesis, plant respiration, and organic matter decomposition, all of which influence the global land–atmosphere carbon flux. For the 20th century, the models show a land–atmosphere carbon flux on the order of −1 Pg of C per yr (i.e., a net sink) for the 1980s and 1990s, with a spread of approximately ±1 Pg of C per yr. These values, which do not account for the additional carbon source due to land-use change, are broadly comparable with various estimates of the "residual terrestrial sink" during the same period (10) (Fig. 1). The spread of estimates increases over time and is greatest for the >3°C case. For <2°C, the sink persists throughout the 21st century. For 2–3°C, the sink increases up to the midcentury, then declines. For >3°C, the sink increases (but less strongly), then declines to zero but with large uncertainty (±3.5 Pg of C per yr) by 2100. The risk for the sink to become a source (Table 1) is 13% for <2°C and 10% for 2–3°C but 44% for >3°C. The slightly lower risk for 2–3°C compared with <2°C is a result of CO_2 fertilization (10), which in this range still has some capacity to mitigate effects of climate change on terrestrial carbon uptake (the increase in photosynthetic uptake due to higher-atmospheric CO_2 is larger than the increase in ecosystem respiration due to the warming) (11, 12). However, the CO_2 fertilization effect saturates at higher CO_2 levels and is then partly offset by higher degrees of global warming, which is reflected by a 44% risk of a terrestrial carbon source for >3°C warming. This result implies a substantial risk that terrestrial uptake of anthropogenic CO_2 will cease if global warming is >3°C, producing an additional positive feedback (12, 13). Assuming a weaker CO_2 fertiliza-

Conflict of interest statement: No conflicts declared.

This paper was submitted directly (Track II) to the PNAS office.

Abbreviations: LPJ, Lund–Potsdam–Jena; PFT, plant functional type.

†To whom correspondence should be addressed. E-mail: marko.scholze@bristol.ac.uk.

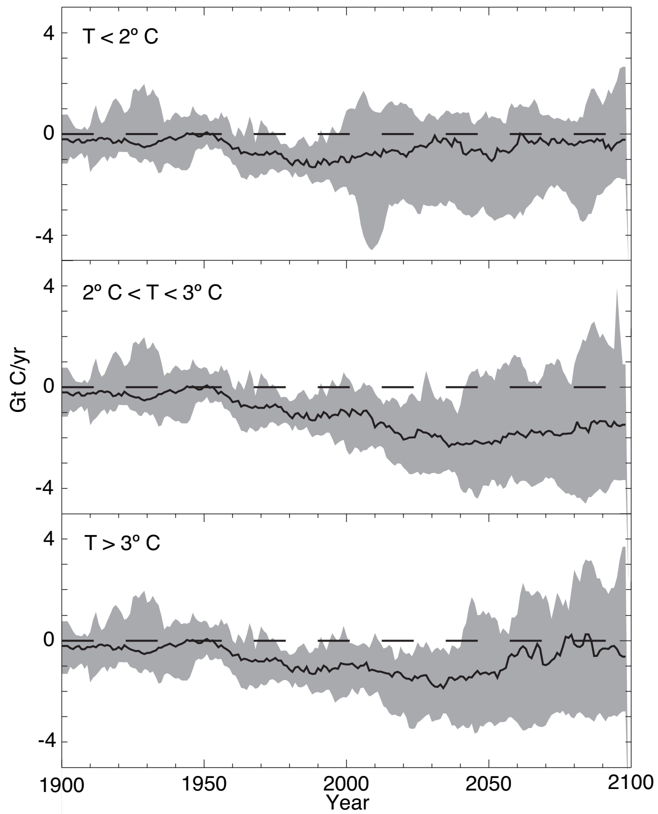

Fig. 1. Median (solid line) and range of the simulated global land–atmosphere carbon flux for three levels of global warming (calculated as the increase in global mean surface temperature between 1961–1990 and 2071–2100). For the years 1900–2000, all 52 model runs are included in each warming level; after the year 2000, only the respective model runs are included in the different warming ranges. The time series have been smoothed by a 10-yr running mean.

tion in the vegetation model would further increase the risks for the land biosphere to become a CO_2 source, however, LPJ's CO_2 fertilization lies within recent observational evidence (10, 14). One of the reasons for the large spread in the results may be differences in simulated tropical precipitation changes (15).

Generally, geographic patterns of risk are similar, but the magnitude of risk increases with the degree of climate change (Fig. 2). However, some geographic features appear only in the warmer scenarios. Also, some of the patterns we show have been observed in earlier work (16–18); however, those studies were mapping total changes rather than the risks of the change in some of the ecosystem properties. Widespread increases in runoff north of 50°N are shown with probabilities as high as 50% even for <2°C, rising to >70% for >3°C. Other areas with high probability of increased runoff are northwestern South America and tropical Africa. Some regions, however, have a high risk of reduced runoff. Models differ in the sign of projected runoff changes over Amazonia, but for >3°C, the probability of reduction exceeds that of increase. A similar result is found for Central America, the eastern seaboard of North America, and the interior of China. The risk of decreased runoff is more pronounced at higher degrees of warming, in particular for >3°C. Southern Europe, West Africa, and the Middle East are also at risk from drought. These results are broadly consistent with changes in runoff simulated for different climate models in other studies (19). Risks of changes in fire frequency are also widespread. Fire frequency partly depends on fuel type and availability, and its relationship to runoff is not straightforward. Reduced fire frequency, reflecting wetter conditions, is indicated for parts of the boreal region, but increased tree cover in some other parts (especially eastern Canada) promotes fire. Reduced fire frequency accompanies increased runoff in tropical Africa. Most semiarid regions, including the Sahel, central Australia, central Asia, southern Africa, and the western U.S., show a high probability of increased wildfires, especially for >3°C, reflecting increased biomass growth. Increased fire risk is also apparent in the southeastern U.S. and at high elevations (notably the Tibetan plateau). More frequent wildfires are likely (>60% for >3°C) in much of South America. Fire is a major factor in structuring vegetation (20), and some biome shifts follow these changes in fire regime, whereas others are forced directly by climate. Forests extend with high probability into the Arctic and into semiarid savannas. Extant forests are destroyed with high probability in parts of the southern boreal zone (especially southern Siberia, the Russian Far East, and the western interior of Canada) and with lower probability in eastern China, Central America, Amazonia, and the Gulf Coast of the U.S. The risks of forest losses in some parts of Eurasia, Amazonia, and Canada are >40% for >3°C.

Table 1. Percentage of scenario runs resulting in a land biosphere carbon source for two time periods

Time period	$T < 2$°C	2°C $< T <$ 3°C	$T > 3$°C
2035–2065	19	0	13
2071–2100	13	10	44

Values (%) were determined by the following: mean over 30 yr > 0.1 Pg of C per yr.

Climate model simulations beyond 2100 examine the "committed" climate change at that time. Here, committed climate change is the climate change associated with the changes in atmospheric composition according to the chosen scenario (A1B, A2, or B1) to 2100 and then held constant from 2100 and the associated trends in ocean temperature and ocean volume due to the ocean thermal inertia. In addition to the ocean inertia, the LPJ runs show the effects of a delay in vegetation responses to climate change (12). The spatial patterns of risk are generally similar, but the risks in highly vulnerable areas (such as runoff in Amazonia and high latitudes, fire in Amazonia and semiarid regions, and change in ecosystem in Amazonia, North America, and Eurasia) increase through the succeeding 200 yr (data not shown).

From a global perspective, it is of interest to quantify at what level of warming risks to some especially vulnerable ecosystems become more and more large-scale ecosystem risks. We calculated the percentages of model runs showing changes between forest and nonforest affecting nonmanaged land area according to the Global Land Cover 2000 product (21). Table 2 shows the risks of change for two different regions of the world (tropical Latin America and boreal northern latitudes). Globally, risks of change in forest to nonforest biome or vice versa to some ecosystems (≥5% land area) are ≥43% for <2°C and increasing to 75% and 88% for 2–3°C and >3°C, respectively. A probability of climate change affecting a larger fraction of the world's ecosystems (≥10% land area) sifting from forests to grassland or vice versa is only apparent for the highest degree of warming, reaching 13% for >3°C. However, this nonforest/forest change is a rather drastic change in habitat and thus a very conservative measure of ecosystem vulnerability; more subtle changes (for instance, changes within forest biome types) will certainly affect a larger fraction (≥10% land area) already at lower degrees of global warming. Beyond the 21st century, the risks continue to increase: e.g., for 2–3°C the risk of change affecting 10% of the land sur-

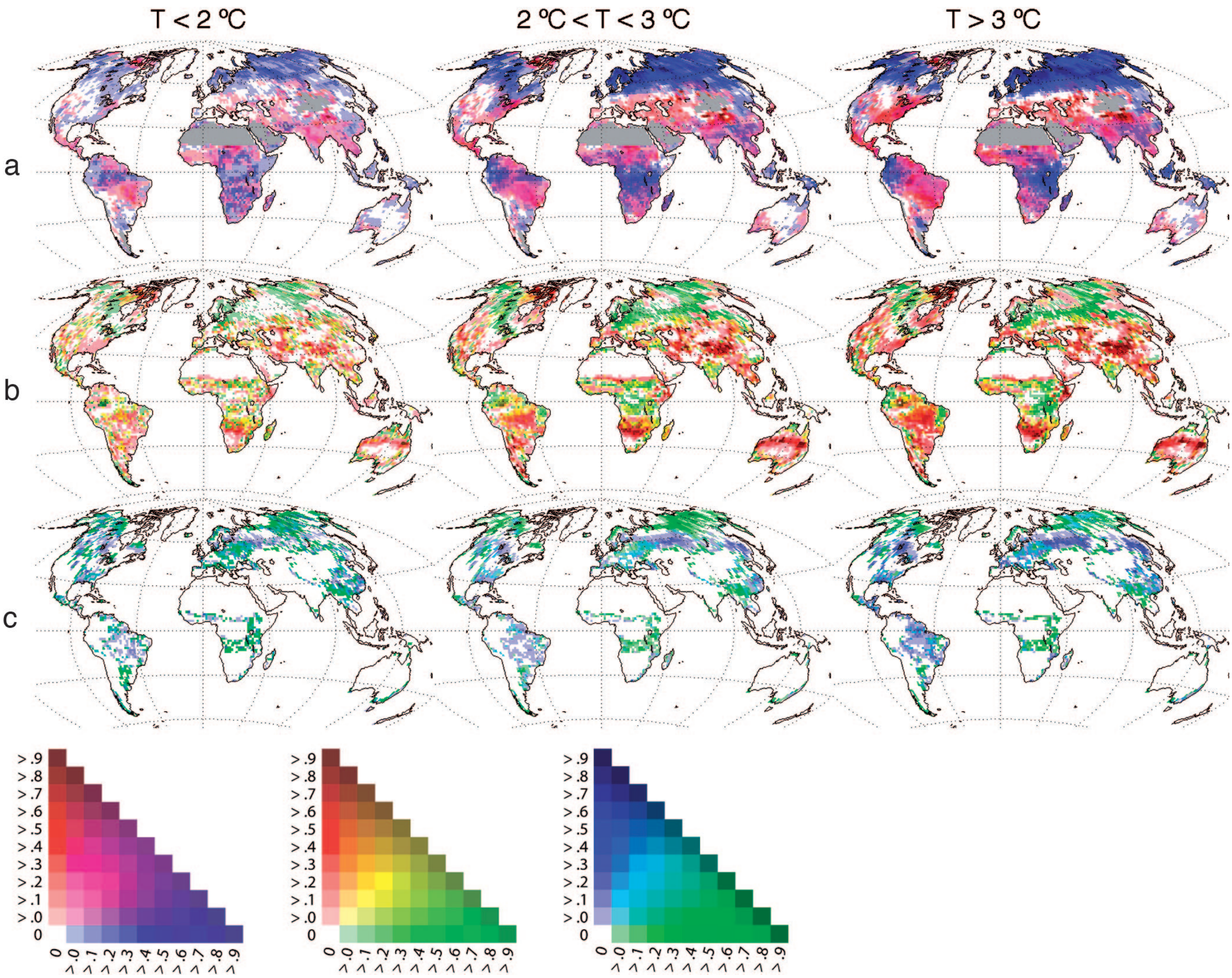

Fig. 2. Probability of exceeding critical levels of change between 1961–1990 and 2071–2100 for three levels of global warming. For quantitative variables (freshwater runoff and wildfire frequency), critical change is defined where the change in the mean of 2071–2100 exceeds $\pm 1\sigma$ of the observed (1961–1990) interannual variability. (*a*) Freshwater runoff (blue for increase, red for decrease; mixed colors show cases where different runs produce changes in opposite directions, i.e., there are runs of both exceeding the critical level by $+1\sigma$ as well as by -1σ). Gray areas denote grid cells with $\leq$10 mm·yr^{-1} mean runoff for 1961–1990. (*b*) Wildfire frequency (red, increase; green, decrease). (*c*) Biome change from forest to nonforest (blue) or vice versa (green). For wildfire frequency and biome change, colors are shown only for grid cells with <75% cultivated and managed areas.

face increases from 0% to 12% a century later, reflecting the combined inertia of ecosystems and climate (data not shown).

Table 2. Percentage of scenario runs showing a shift from forest to nonforest vegetation or vice versa

	Tropical Latin America			Boreal northern latitudes		
Global warming range	5%	10%	20%	5%	10%	20%
$T > 3$°C	56	38	12	100	88	31
2°C $< T <$ 3°C	25	20	0	100	70	10
$T < 2$°C	19	19	0	75	44	0

Values are the percentages of scenario runs representing a shift from forest to nonforest vegetation (or vice versa) affecting a minimum area specified by the given percentage values (5%, 10%, and 20%) of the total noncultivated land area for two different regions (tropical Latin America and boreal northern latitudes).

Discussion

Although natural ecosystems have been extensively modified (22) in the past, the indicators adopted here are conservative and should be robust in their application from natural to managed landscapes. For example, a shift from potential forest to a grassland biome implies a change in the kinds of land use that can be practiced. The major areas at risk of potential forest loss are predominantly forested today, i.e., they have not been subject to forest clearance up to now. A shift from nonforest to forest also has implications for biodiversity, because many species are adapted to treeless conditions. Our analysis can be expected to underestimate the risks to biodiversity because more subtle shifts in the dominance of different plant functional types (PFTs) have been disregarded. Decreasing runoff implies that extra effort and expense may be required to meet people's demand for water, even if this demand does not increase. Increasing runoff helps freshwater availability but may carry with it an increased flood risk in susceptible regions. Any increase in wildfire frequency represents a hazard to lives and property in any region where people and (semi-)natural vegetation coexist.

An analysis of the implications of climate-induced changes in ecosystems for human activities would be more complex and would include consideration of impacts on crop production, regionally specific information on social and economic drivers of land use, and demographic and economic trends. Also, the climate-induced changes in ecosystems occur concurrent with human-induced changes. These human-driven transitions in ecosystems are likely to have a larger impact on ecosystems than climate-only-induced transitions (23). We have made an attempt to quantify the underlying risks assuming that local populations and regional institutions are adapted to recent interannual variability. A risk is thus assumed only when the frequency of "extreme" years increases by an order of magnitude. Using this criterion and a conservative criterion for biome shifts, several strong conclusions emerged. (*i*) Nontrivial risks are associated with global warming $<2°C$. (*ii*) Greater global warming produces greater risks: Risks already manifest for $<2°C$ become greater for 2–3°C and again for $>3°C$. (*iii*) The risk of large-scale biome shifts depends strongly and nonlinearly on the degree of warming. (*iv*) Amazonia and the circumpolar boreal and Arctic regions emerge as especially vulnerable; Amazonia is at risk from drought, climate-induced forest dieback, and wildfire; parts of the boreal forest may be lost; and the Arctic tundra is at risk from forest invasion. (*v*) Some geographic patterns of risk first appear when global warming is $>3°C$. Although this information cannot provide an unambiguous definition of dangerous climate change, it may help to inform policy discussions by drawing attention to the steeply increasing risks to ecosystem services associated with global climate changes beyond the range to which the climate system is already committed.

Materials and Methods

The general circulation model outputs represent four emission scenarios: "committed" climate change (i.e., atmospheric composition held constant from 2000), and Special Report on Emission Scenarios A1B, A2, and B1 (24). All of the climate model runs were initialized for preindustrial conditions and run up to 2000 with radiative forcing based on observations and then to 2100 under one of the four scenarios. Some were continued until 2200 or 2300 with atmospheric composition held constant from 2100. To circumvent the problems of differing climate sensitivity among the models or the need to assign probabilities to scenarios (25), we classified the climate model runs into three groups according to the simulated increase in global mean surface temperature between 1961–1990 and 2071–2100: $<2°C$ (16 runs), 2–3°C (20 runs), and $>3°C$ (16 runs) (see Table 3, which is published as supporting information on the PNAS web site). We made a simple approximation of the probability density function within each group by assigning equal weight to each model run.

The LPJ dynamic global vegetation model (8, 9) combines process-based descriptions of terrestrial ecosystem structure (vegetation composition, biomass, and height) and function (energy absorption and carbon cycling). Vegetation composition is described by 10 different PFTs, which are distinguished according to their bioclimatic (boreal, temperate, or tropical), physiological (C3 or C4 photosynthesis), morphological (tree or grass), and phenological (deciduous or evergreen) attributes. The model runs on a regular latitude–longitude grid (here at 1.5° resolution) with atmospheric CO_2 concentration, soil texture, and monthly fields of temperature, precipitation, and fractional sunshine hours as input. The fractional coverage of a PFT within a grid-cell depends on its specific environmental limits and on resource competition among the PFTs. Photosynthesis is calculated by a Farquhar–Collatz (26, 27) scheme coupled to a two-layer soil-water model (28) on a daily basis. Assimilated CO_2 is allocated to four different tissue pools (leaves, sap- and heart-wood, and roots) on an annual basis. Soil and litter C pools are updated monthly, and decomposition rates depend on soil temperature and soil moisture (29). Vegetation dynamics are simulated annually based on the productivity of the different PFTs as well as on disturbance, mortality, and establishment. Natural disturbance is included by computing fire occurrence as a function of a threshold litter load, surface soil moisture, and temperature (30) on a yearly time step. The simulated abundances of the PFTs modeled by LPJ are used to assign grid cells to forest and nonforest biome types according to their fractional plant cover (fractional plant cover of woody PFTs > 0.2 for forest) and stand height h ($h > 7$ m for forest). The assignment algorithm is as described in ref. 31; however, we used a minimum stand height of 7 m for forest biomes (instead of 10 m as in ref. 31) because the LPJ version used here (9) has an improved hydrological model, which produces lower vegetation heights under drier conditions transitional between forests and nonforests. The assignment was based on 30-yr mean values. Climate input data for LPJ were calculated by using anomalies of monthly mean temperature, precipitation, and cloud cover from the 52 climate experiments. Climate anomalies were defined as differences from the 30-yr mean for the baseline period, 1961–1990, in the 20th-century model simulations. They were applied to a baseline climatology from the Climate Research Unit (1961–1990) (32). LPJ was spun up by repeating a 30-yr cycle (1890–1920) of climate anomalies over a 1,000-yr simulation period. To capture physiological effects of rising CO_2, we also provided LPJ with the time series of global mean CO_2 concentrations from observations (33, 34) and from the Special Report on Emission Scenarios (24) for the future. LPJ has been extensively tested (8, 9, 35) and applied in several case studies (36–39) and intercomparison projects (12, 38).

We assumed that the risks of critical change for wildfire frequency and change in ecosystem type apply to nonmanaged land areas; thus, we applied the Global Land Cover 2000 product (21) to mask out grid cells with 75% or more cultivated or managed area. We defined critical change based on the difference between the 2071–2100 and the 1961–1990 means. For wildfire frequency and runoff, we defined critical change when the change in the mean exceeded $\pm 1\sigma$ of the natural interannual variability during 1961–1990, based on LPJ simulations using climate observations (32). For an extreme event occurring once every 100 yr, a shift in the mean by 1σ in the direction of the extreme translates into an $\approx$10-fold increase in its frequency: The "100-yr event" becomes the "10-yr event". Thus, our analysis focuses on the risk of impacts of changes in extreme events on ecosystems as opposed to the significance of long-term mean climate change (40). For changes in ecosystem type, we conservatively defined critical change as a shift between forest and nonforest states. We also analyzed globally aggregated changes in the carbon balance of ecosystems, defining critical change when the 30-yr mean terrestrial carbon source exceeds $+0.1$ Pg of C per yr [corresponding to a total source of 3 Pg of C, which is slightly more than the current absolute value of the annual terrestrial carbon sink (11)].

We thank the international modeling groups for providing their data for analysis; the Program for Climate Model Diagnosis and Intercomparison for collecting and archiving the model data; the Joint Scientific Committee/Climate Variability and Predictability Working Group on Coupled Modeling and their Coupled Model Intercomparison Project and Climate Simulation Panel for organizing the model data analysis activity; and the Intergovernmental Panel on Climate Change (IPCC) WG1 TSU for technical support. We also thank S. Cornell, J. House, W. Lucht, and S. Schaphoff for discussions. The IPCC Data Archive at Lawrence Livermore National Laboratory is supported by the Office of Science, U.S. Department of Energy.

1. United Nations Framework Convention on Climate Change (1992) *United Nations Framework Convention on Climate Change, United Nations, Rio de Janeiro, 1992* (United Nations Framework Convention on Climate Change, Bonn, Germany). Available at: www.unfccc.int/resource/ccsites/senegal/conven.htm.
2. Parry, M. L., Carter, T. R. & Hulme, M. (1996) *Global Environ. Change* **6,** 1–6.
3. Parmesan, C. & Yohe, G. (2003) *Nature* **421,** 37–42.
4. Houghton, J. T., Ding Y., Griggs, D. J., Noguer, M. van der Linden, P. J. & Xiaosu, D. (2001) *Climate Change 2001: The Scientific Basis* (Cambridge Univ. Press, Cambridge, U.K.).
5. Ahmad, Q. K., Anisimov, O., Arnell, N., Brown, S., Burton, I., Campos, M., Canziani, O., Carter, T., Cohen, S. J., Desanker, P., *et al.* (2000) *Summary for Policymakers Climate Change 2001: Impacts, Adaptation and Vulnerability* (Cambridge Univ. Press, New York).
6. Mastrandrea, M. D. & Schneider, S. H. (2004) *Science* **304,** 571–575.
7. Schneider, S. H. & Mastrandrea, M. D. (2005) *Proc. Natl. Acad. Sci. USA* **102,** 15728–15735.
8. Sitch, S., Smith, B., Prentice, I. C., Arneth, A., Bondeau, A., Cramer, W., Kaplan, J. O., Levis, S., Lucht, W., Sykes, M. T., *et al.* (2003) *Global Change Biol.* **9,** 161–185.
9. Gerten, D., Schaphoff, S., Haberlandt, U., Lucht, W. & Sitch, S. (2004) *J. Hydrol.* **286,** 10.1016/j.jhydrol.2003.09.029.
10. Norby, R. J., DeLucia, E. H., Gielen, B., Calfapietra, C., Giardina, C. P., King, J. S., Ledford, J., McCarthy, H. R., Moore, D. J. P., Ceulemans, R., *et al.* (2005) *Proc. Natl. Acad. Sci. USA* **102,** 18052–18056.
11. Prentice, I. C., Farquhar, G. D., Fasham, M. J. R., Goulden, M. L., Heimann, M., Jaramillo, V. J., Kheshgi, H. S., Le Quéré, C., Scholes, R. J., Wallace, D. W. R., *et al.* (2001) in *Climate Change 2001: The Scientific Basis*, eds. Houghton, J. T., Ding Y., Griggs, D. J., Noguer, M. van der Linden, P. J. & Xiaosu, D. (Cambridge Univ. Press, Cambridge, U.K.), pp. 183–237.
12. Cramer, W., Bondeau, A., Woodward, F. I., Prentice, I. C., Betts, R. A., Brovkin, V., Cox, P. M., Fisher, V., Foley, J. A., Friend, A., *et al.* (2001) *Global Change Biol.* **7,** 357–373.
13. Cox, P. M., Betts, R. A., Jones, C. D., Spall, S. A. & Totterdell, I. J. (2000) *Nature* **408,** 184–187.
14. Prentice, I. C., Bondeau, A., Cramer, W., Harrison, S. P., Hickler, T., Lucht, W., Sitch, S., Smith & Sykes, M. T. (2007) in *Terrestrial Ecosystems in a Changing World*, IGBP Book Series, eds. Canadell, J., Pitelka, L. & Pataki, D. (Springer, Heidelberg, Germany), in press.
15. Schaphoff, S., Lucht, W., Gerten, D., Sitch, S., Cramer, W. & Prentice, I. C. (2006) *Climate Change* **74,** 97–122.
16. Neilson, R. P., Prentice, I. C., Smith B., Kittel, T. & Viner, D. (1998) in *IPCC Special Report on The Regional Impacts of Climate Change*, eds. Watson, R. T., Zinyowera, M. C. & Moss, R. H. (Cambridge Univ. Press, Cambridge, U.K.), Annex C.
17. Neilson, R. P. & Drapek, R. J. (1998) *Global Change Biol.* **4,** 505–521.
18. Bachelet, D., Neilson, R. P., Lenihan, J. M. & Drapek, R. J. (2001) *Ecosystems* **4,** 164–185.
19. Arnell, N. W. (2003) *Hydrol. Earth Syst. Sci.* **7,** 619–641.
20. Bond, W. J., Woodward, F. I. & Midgley, G. F. (2005) *New Phytol.* **165,** 525–538.
21. European Commission, Joint Research Centre (2003) *Global Land Cover 2000 Database*. Available at: www-gvm.jrc.it/glc2000.
22. Foley, J. A., DeFries, R., Asner, G. P., Barford, C., Bonan, G., Carpenter, S. R., Chapin, F. S., Coe, M. T., Daily, G. C., Gibbs, H. K., *et al.* (2005) *Science* **309,** 570–574.
23. Schröter D., Cramer, W., Leemans, R., Prentice, I. C., Araújo, M. B., Arnell, N. W., Bondeau, A., Bugmann, H., Carter, T. R., Gracia, C. A., *et al.* (2005) *Science* **310,** 1333–1337.
24. Nakicenovic, N., Davidson, O., Davis, G., Grübler, A., Kram, T., La Rovere, E. L., Metz, B., Morita, T., Pepper, W., Pitcher, H., *et al.* (2000) *Special Report on Emission Scenarios* (Cambridge Univ. Press, New York).
25. Schneider, S. H. (2001) *Nature* **411,** 17–19.
26. Farquhar, G. D., von Caemmerer, S. & Berry, J. A. (1980) *Planta* **149,** 78–90.
27. Collatz, G. J., Ribas-Carbo, M. & Berry, J. A. (1992) *Austr. J. Plant Physiol.* **19,** 519–538.
28. Haxeltine, A. & Prentice, I. C. (1996) *Global Biogeochem. Cycl.* **10,** 693–709.
29. Lloyd, J. & Taylor, J. A. (1994) *Funct. Ecol.* **8,** 315–323.
30. Thonicke, K., Venevsky, S., Sitch, S. & Cramer, W. (2001) *Glob. Ecol. Biogeogr.* **10,** 661–677.
31. Joos, F., Gerber, S., Prentice, I. C., Otto-Bliesner, B. L. & Valdes, P. J. (2004) *Glob. Biogeochem. Cycl.* **18,** 10.1029/2003GB002156.
32. New, M., Hulme, M. & Jones, P. (1999) *J. Climate* **12,** 829–856.
33. Etheridge, D. M., Steele, L. P., Langenfelds, R. L., Francey, R. J., Barnola, J.-M. & Morgan, V. I. (1996) *J. Geophys. Res.* **101,** 4115–4128.
34. Keeling, C. D. & Whorf, T. P. (1994) in *Trends '93: A Compendium of Data on Global Change*, eds. Boden, T., Kaiser, D. P., Sepanski, R. J. & Stoss, F. W. (Carbon Dioxide Information Analysis Center, Oak Ridge Natl. Lab., Oak Ridge, TN), ORNL/CDIAC65.
35. Wagner, W., Scipal, K., Pathe, C., Gerten, D., Lucht, W. & Rudolf, B. (2003) *J. Geophys. Res.* **108,** 10.1029/2003JD003663.
36. Prentice, I. C., Heimann, M. & Sitch, S. (2000) *Ecol. Appl.* **10,** 1553–1573.
37. Lucht, W., Prentice, I. C., Myneni, R. B., Sitch, S., Friedlingstein, P., Cramer, W., Bousquet, P., Buermann, W. & Smith, B. (2002) *Science* **296,** 1687–1689.
38. McGuire, A. D., Sitch, S., Clein, J. S., Dargaville, R., Esser, G., Foley, J., Heimann, M., Joos, F., Kaplan, J., Kicklighter, D. W., *et al.* (2001) *Global Biogeochem. Cycles* **15,** 183–206.
39. Scholze, M., Knorr, W. & Heimann, M. (2003) *Holocene* **13,** 327–333.
40. Hulme, M., Barrow, M. E., Arnell, N. W., Harrison, P. A., Johns, T. C. & Downing, T. E. (1999) *Nature* **397,** 688–691.

Supplementary Information to: A climate change risk analysis for world ecosystems

Table S1: Models and scenarios used in this study and the global mean temperature difference between 2071-2100 and 1961-1990 used to categorize the model run into one of the three global warming groups, as well as the mean land-atmosphere C flux over 2071-2100 as simulated by LPJ.

Model name	**Scenario**	**ΔT (2071-2100 – 1961-1990) in °C**	**Mean land-atm. C flux (2071-2100) in Pg C/yr**
Canadian Centre for Climate Model. & Analysis: CGCM3.1(T47) (1)	B1	2.1	-1.3
Météo-France / Centre National de Recherches Météorologiques: CNRM-CM3 (2)	A1B	3.1	-2.6
	A2	3.8	-2.2
	B1	2.0	-2.0
	committed	0.6	-0.3
CSIRO Atmospheric Research: CSIRO-Mk3.0 (3)	A1B	2.3	-2.7
	A2	2.9	-3.0
	B1	1.3	-1.7
US Dept. of Commerce / NOAA / Geophysical Fluid Dynamics Laboratory: GFDL-CM2.0 (4)	A1B	3.2	-0.2
	A2	3.5	1.3
	B1	2.4	-0.3
	committed	1.2	0.0
US Dept. of Commerce / NOAA / Geophysical Fluid Dynamics Laboratory: GFDL-CM2.1 (5)	A1B	2.8	-0.5
	A2	3.3	0.9
	B1	2.0	-0.7
	committed	0.9	0.9
NASA / Goddard Institute for Space Studies: GISS-AOM (6)	A1B	2.2	-2.2
	B1	1.6	-1.1
NASA / Goddard Institute for Space Studies: GISS-EH (7)	A1B	2.2	-1.8
NASA / Goddard Institute for Space Studies: GISS-ER (8)	A1B	2.4	-1.8
	A2	2.8	-1.2
	B1	1.7	-1.4
	committed	0.02	-0.5
Institute for Numerical Mathematics: INM-CM3.0 (9)	A1B	3.1	-1.8
	A2	3.8	-0.5
	B1	2.5	-0.8
Institut Pierre Simon Laplace: IPSL-CM4 (10)	A1B	3.4	0.5
	A2	3.9	1.3
	B1	2.6	0.4
	committed	1.1	-0.2
Center for Climate System Research (University of Tokyo), NIES, and Frontier Research Center for Global Change: MIROC3.2(medres) (11)	A1B	3.6	-1.9
	A2	4.0	-2.4
	B1	2.5	-0.2
	committed	0.8	-0.3
Max Planck Institute for Meteorology: ECHAM5/MPI-OM (12)	A1B	3.6	-0.9
	A2	3.9	0.2

	B1	2.6	-0.6
	committed	0.6	0.0
Meteorological Research Institute: MRI-CGCM2.3.2 (13)	A1B	2.6	-2.4
	A2	2.9	-2.7
	B1	1.9	-1.6
	committed	0.9	0.0
National Center for Atmospheric Research: CCSM3 (14)	A1B	3.3	-2.7
	B1	2.1	-2.0
National Center for Atmospheric Research: PCM (15)	A1B	2.5	-3.2
	A2	2.7	-4.1
	B1	1.7	-2.0
	committed	0.8	0.3
Hadley Centre for Climate Prediction and Research / Met Office: UKMO-HadCM3 (16)	A1B	3.4	0.4
	A2	3.8	1.9
	B1	2.4	1.1
	committed	0.7	-0.4

Supplementary References

1. Flato, G. M. & Boer, G. J. (2001) *Geophys. Res. Lett.* **28**, 195.

2. Salas-Mélia, D. et al. (2005) in preparation for *Clim. Dynamics*.

3. Gordon, H. B. et al. (2002) The CSIRO Mk3 climate system model. CSIRO Atmospheric Research technical paper no. 60, CSIRO Atmospheric Research, Aspendale. 130 pp.

4. Delworth, T. L. et al. (2004) submitted to *J. Climate* (2004).

5. Russell, G. L., Miller, J. R. & Rind, D. (1995) *Atmosphere-Ocean* **33**, 683.

6. Schmidt, G. A. et al. (2005) *J. Climate*, in press.

7. Diansky, N. A. & Volodin, E. M. (2002) *Izv. Atmos. Ocean. Phys.* (Engl. Transl.) **38**, 732.

8. Marti, O. et al. (2004) The new IPSL climate system model: IPSL-CM4, Note du Pôle de Modélisation n. 26, ISSN 1288-1619, IPSL, Paris.

9. K-1 model developers (2004) K-1 coupled model (MIROC) description, K-1 technical report 1, eds. Hasumi, H. & Emori, S., Center for Climate System Research, University of Tokyo, Tokyo, 34 pp.

10. Jungclaus, J. H. et al. (2005) submitted to *J. Climate*.

11. Yukimoto et al. (2001) *Pap. Meteor. and Geophys.* **51**, 47.

12. Collins, W. D. et al. (2005) submitted to *J. Climate*.

13. Washington, W. M. et al. (2000) *Clim. Dynamics* **16**, 755.

14. Gordon, C. et al. (2000) *Clim. Dynamics* **16**, 147.

Figure Legends:

Figure S1: Exceedence of a threshold one standard deviations of the variability for the period 1961-1990) in the mean over 2071-2100 compared to the mean 1961-1990 for runoff (first column, blue for exceedance above the threshold and red for below) and fire occurrence (second column, green for above and red for below). The third column shows the change in biome type for 2071-2100 compared to 1961-1990 with green being a change from non-forest to forest and blue vice versa. The scenarios displayed produce a global warming of less than 2° C.

Figure S2: As Figure S1 but for scenario runs with a global warming of 2-3°C.

Figure S3: As Figure S1 but for scenario runs with a global warming more than 3°C.

Figure S4: Global land-atmosphere C flux. Dashed lines are same models as solid lines, but for a different scenario.

Figure S1

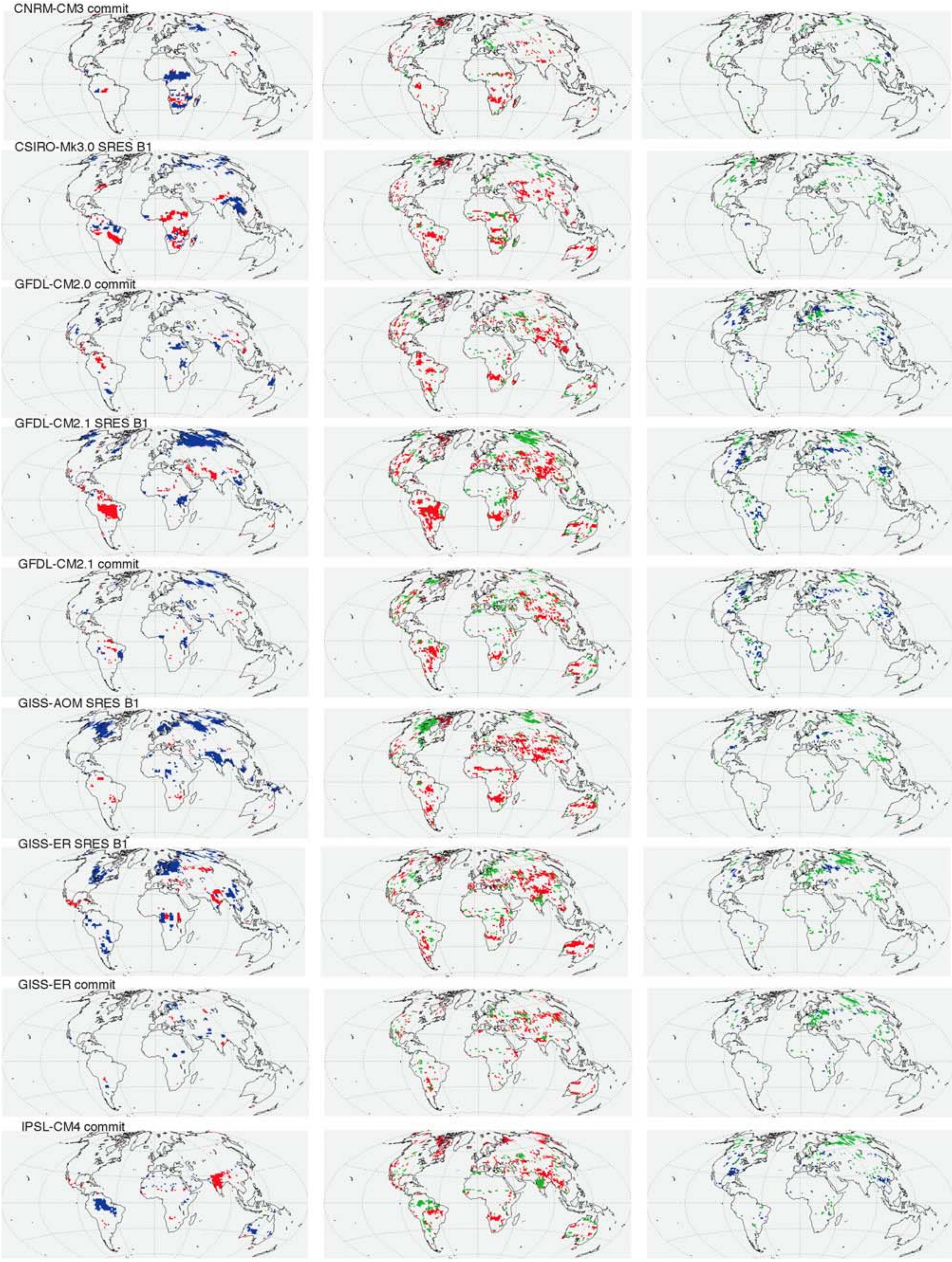
CNRM-CM3 commit
CSIRO-Mk3.0 SRES B1
GFDL-CM2.0 commit
GFDL-CM2.1 SRES B1
GFDL-CM2.1 commit
GISS-AOM SRES B1
GISS-ER SRES B1
GISS-ER commit
IPSL-CM4 commit

Figure S1 cont.

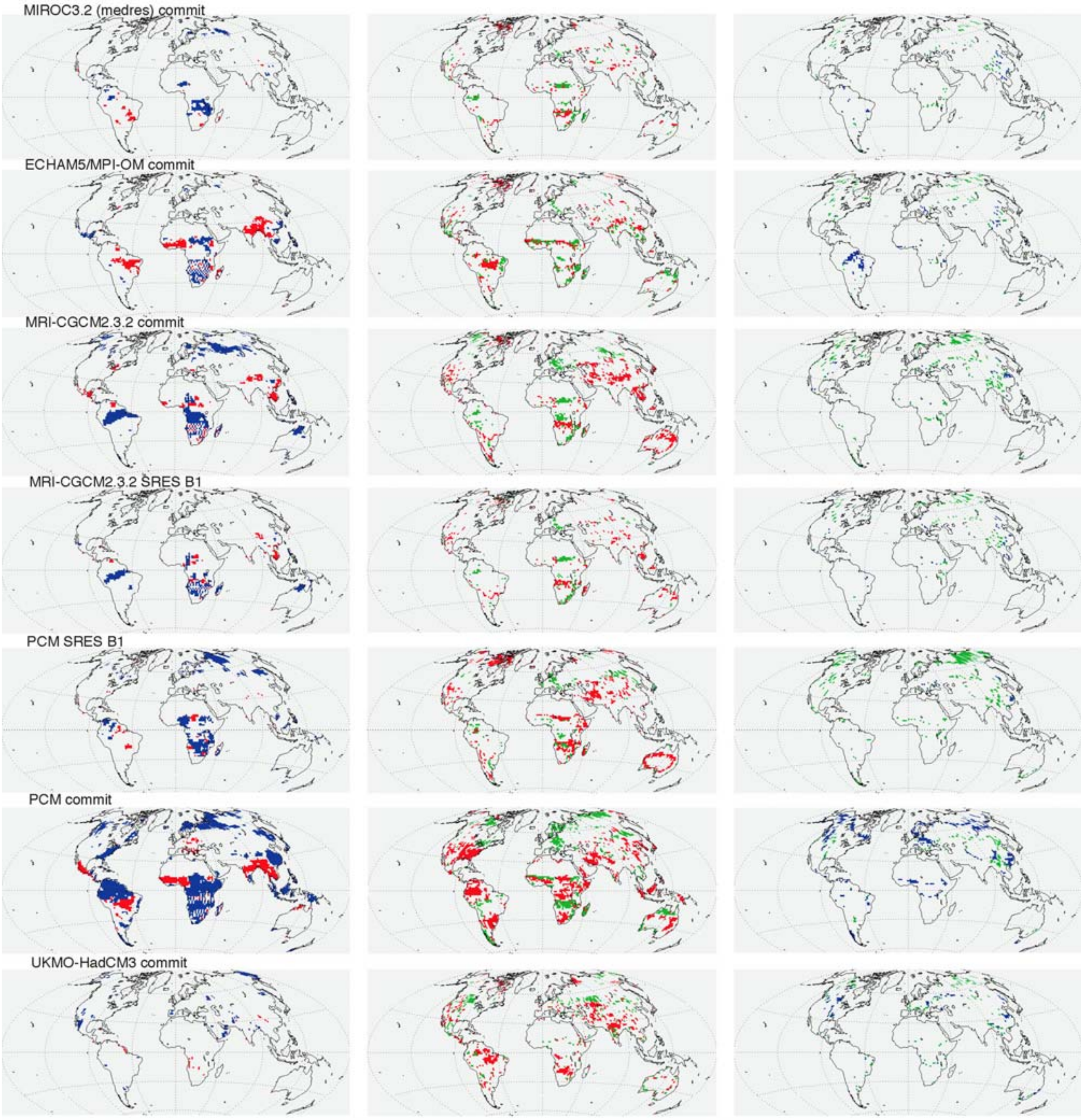

Figure S2

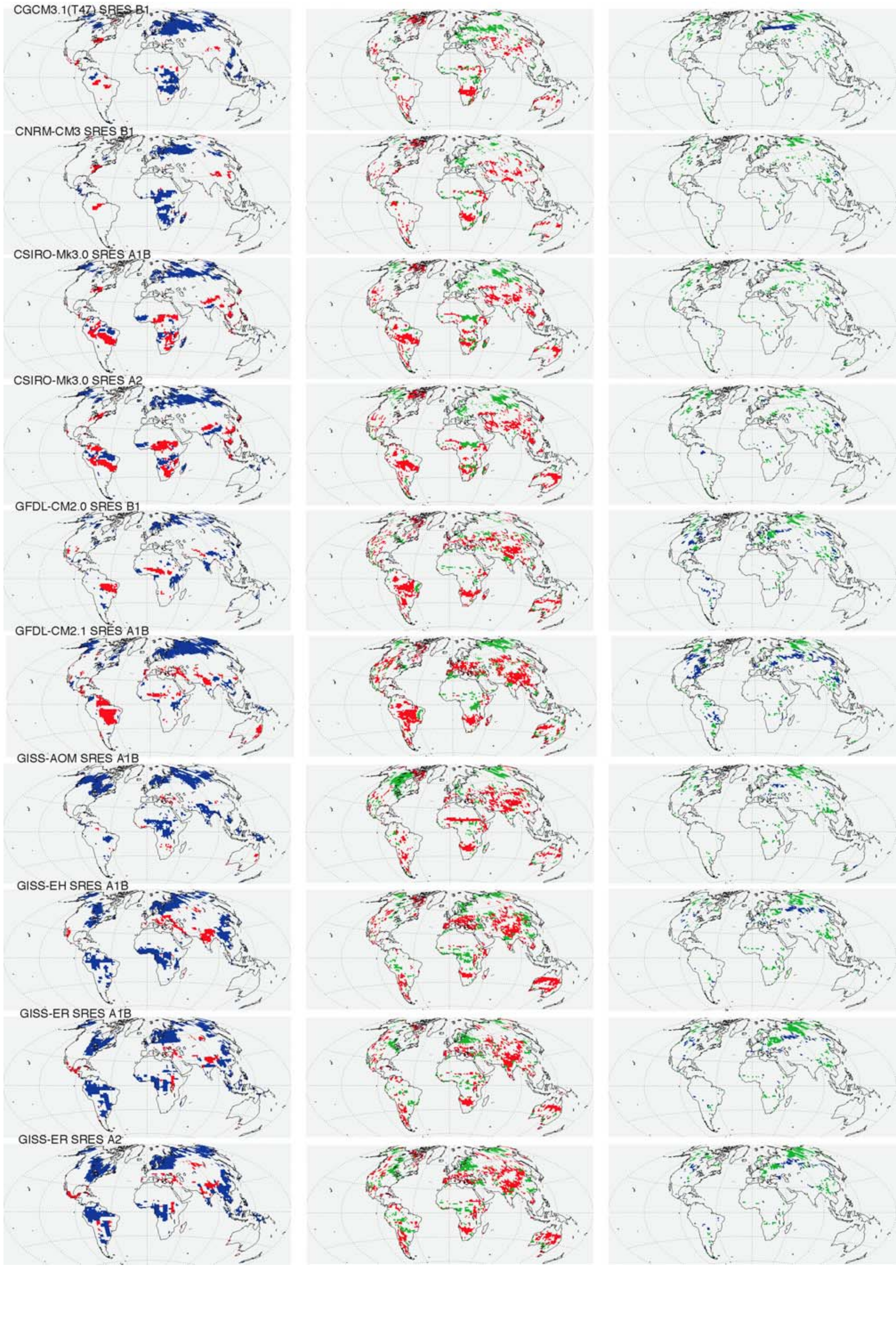
CGCM3.1(T47) SRES B1
CNRM-CM3 SRES B1
CSIRO-Mk3.0 SRES A1B
CSIRO-Mk3.0 SRES A2
GFDL-CM2.0 SRES B1
GFDL-CM2.1 SRES A1B
GISS-AOM SRES A1B
GISS-EH SRES A1B
GISS-ER SRES A1B
GISS-ER SRES A2

Figure S2 cont

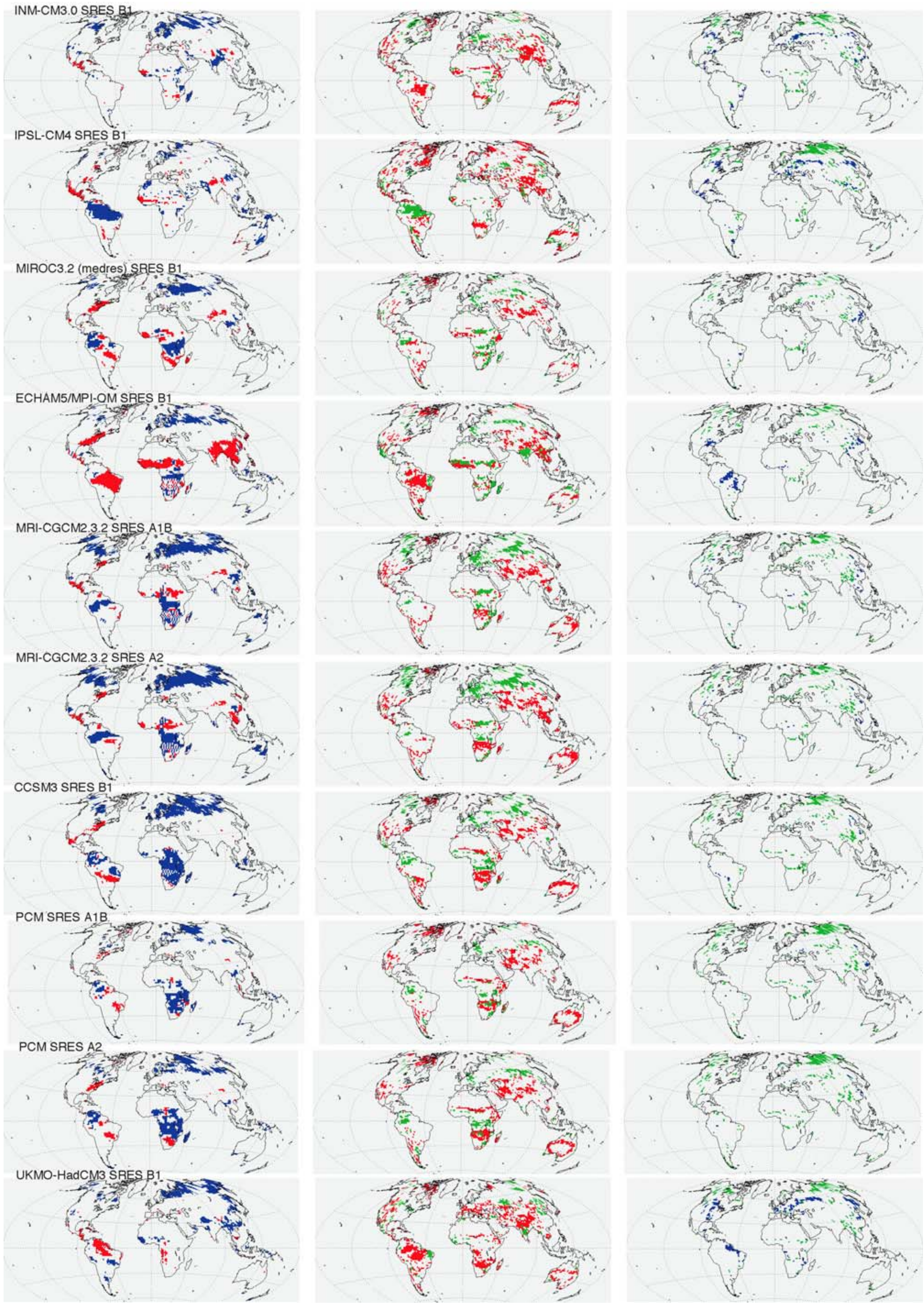

Figure S3

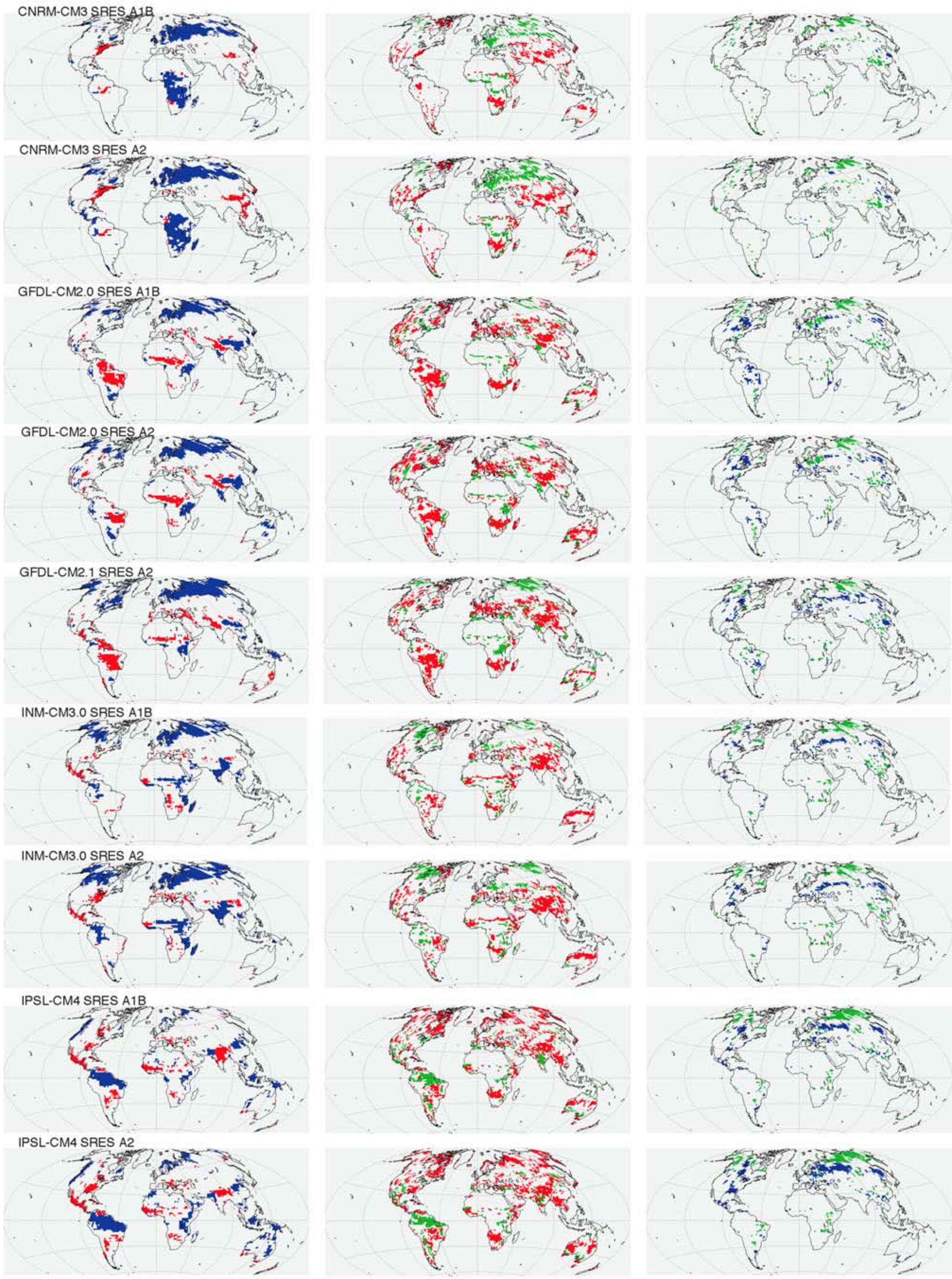
CNRM-CM3 SRES A1B
CNRM-CM3 SRES A2
GFDL-CM2.0 SRES A1B
GFDL-CM2.0 SRES A2
GFDL-CM2.1 SRES A2
INM-CM3.0 SRES A1B
INM-CM3.0 SRES A2
IPSL-CM4 SRES A1B
IPSL-CM4 SRES A2

Figure S3 cont

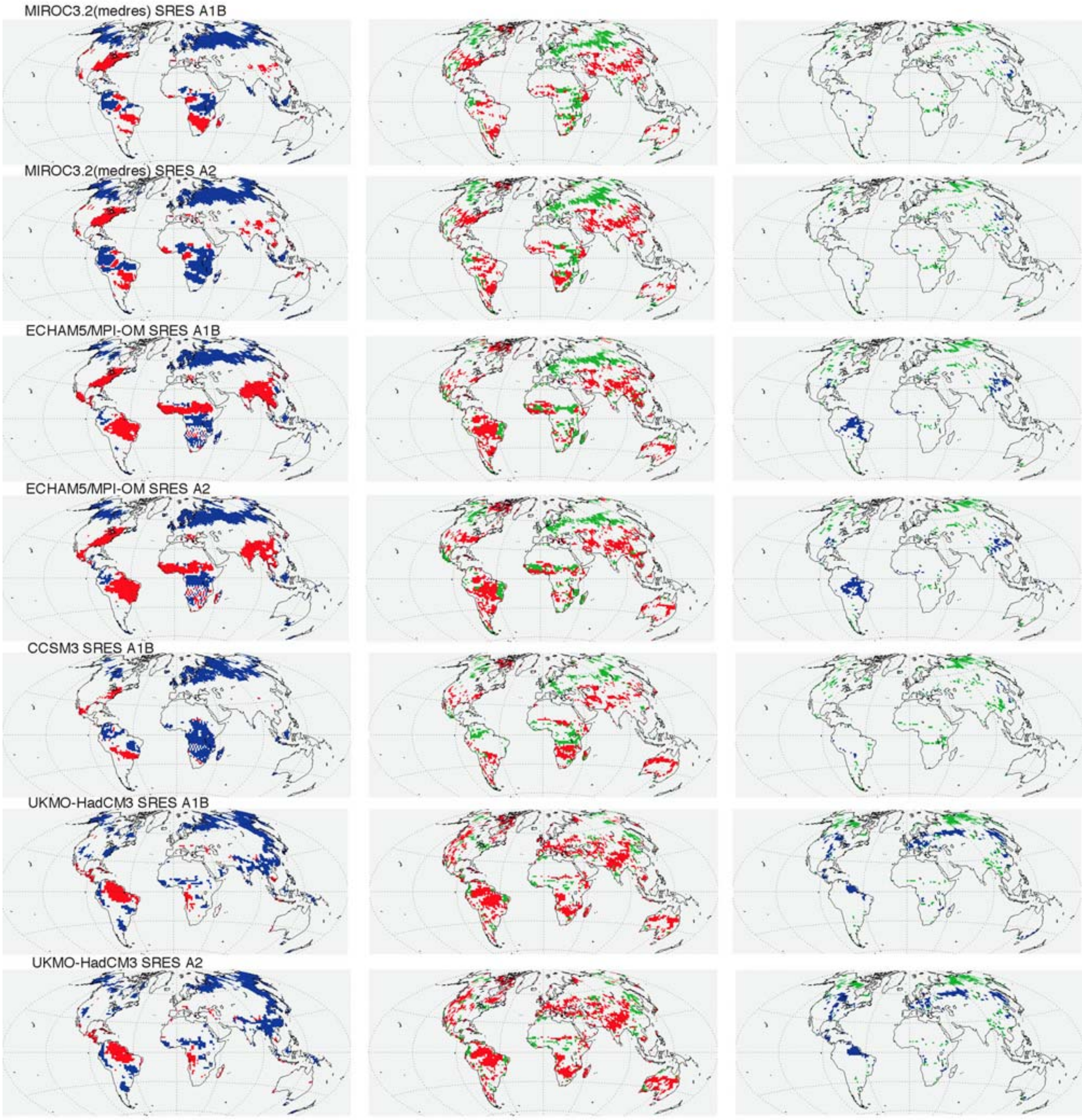

Figure S4

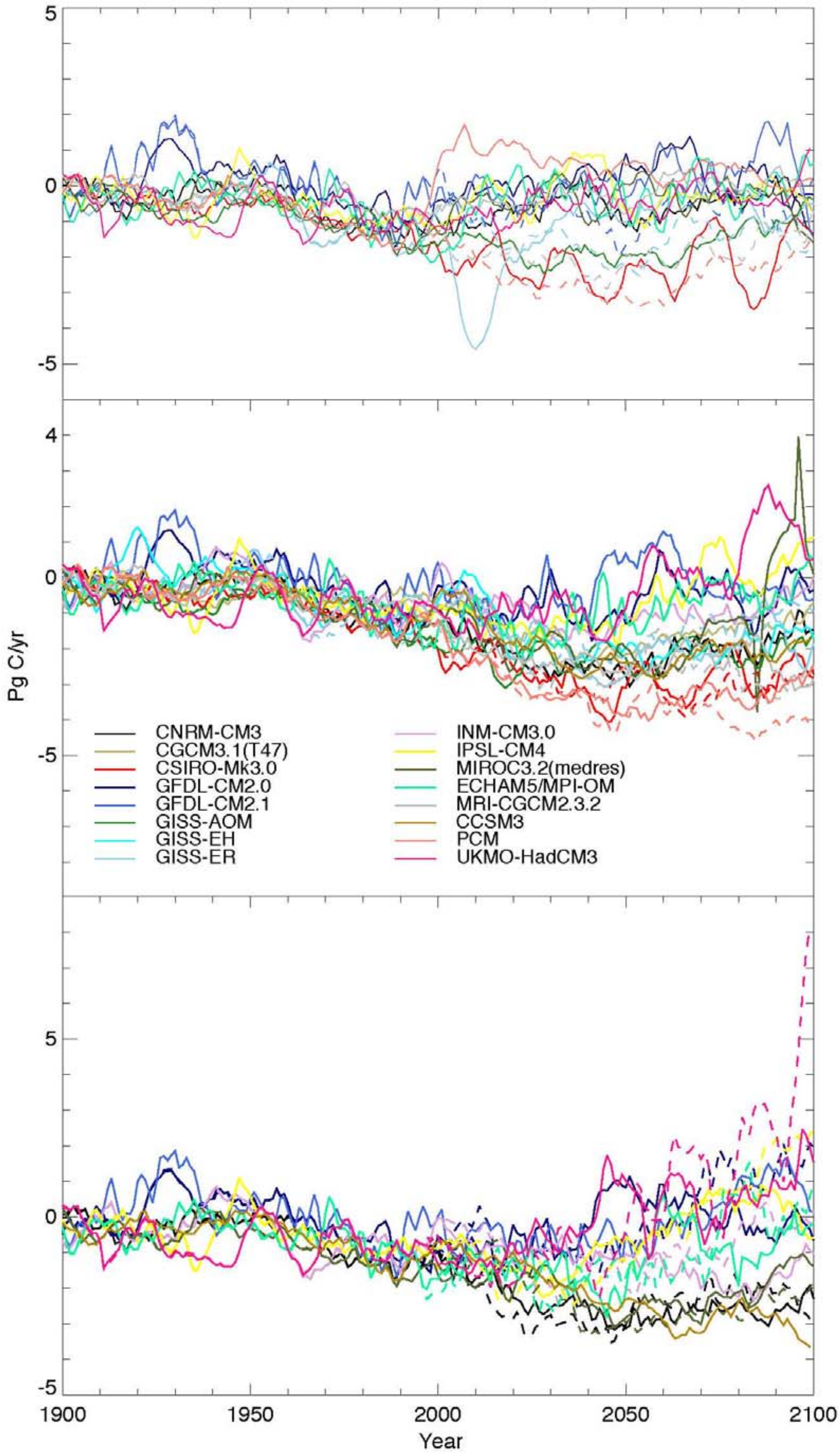

5
0
-5
4
0
-5
5
0
-5
Pg C/yr
CNRM-CM3
CGCM3.1(T47)
CSIRO-Mk3.0
GFDL-CM2.0
GFDL-CM2.1
GISS-AOM
GISS-EH
GISS-ER
INM-CM3.0
IPSL-CM4
MIROC3.2(medres)
ECHAM5/MPI-OM
MRI-CGCM2.3.2
CCSM3
PCM
UKMO-HadCM3
1900
1950
2000
2050
2100
Year